Article

Corresponding Author:

Houman Rokni, Afton Chemical Ltd., Bracknell, Berkshire, RG12 2UW, UK & Department of Mechanical Engineering and Aeronautics, City University of London, Northampton Square, EC1V 0HB London, UK

Email: houman.rokni@aftonchemical.com

General method for prediction of thermal conductivity for well-characterized hydrocarbon mixtures and fuels up to extreme conditions using entropy scaling

Houman B. Rokni [1, 2], Joshua D. Moore[3], Ashutosh Gupta[3], Mark A. McHugh[4], Rajendar R. Mallepally[4] and Manolis Gavaises[2]

[1]Afton Chemical Ltd., Bracknell, Berkshire, RG12 2UW, UK
[2]Department of Mechanical Engineering and Aeronautics, City, University of London, Northampton Square, EC1V 0HB London, UK
[3]Afton Chemical Corp., Richmond, Virginia 23219, USA
[4]Department of Chemical and Life Science Engineering, Virginia Commonwealth University, Richmond, Virginia 23284, USA

Abstract

A general and efficient technique is developed to predict the thermal conductivity of well-characterized hydrocarbon mixtures, rocket propellant (RP) fuels, and jet fuels up to high temperatures and high pressures (HTHP). The technique is based upon entropy scaling using the group contribution method coupled with the Perturbed-Chain Statistical Associating Fluid Theory (PC-SAFT) equation of state. The mixture number averaged molecular weight and hydrogen to carbon ratio are used to define a single pseudo-component to represent the compounds in a well-characterized hydrocarbon mixture or fuel. With these two input parameters, thermal conductivity predictions are less accurate when the mixture contains significant amounts of iso-alkanes, but the predictions improve when a single thermal conductivity data point at a reference condition is used to fit one model parameter. For eleven binary mixtures and three ternary mixtures at conditions from 288 to 360 K and up to 4,500 bar, thermal conductivities are predicted with mean absolute percent deviations (MAPDs) of 16.0 and 3.0% using the two-parameter and three-parameter models, respectively. Thermal conductivities are predicted for three RP fuels and three jet fuels at conditions from 293 to 598 K and up to 700 bar with MAPDs of 14.3 and 2.0% using the two-parameter and three-parameter models, respectively.

Introduction

Advanced computational fluid dynamics (CFD) approaches have been utilized to simulate the performance of fuel injection equipment systems and to investigate phenomena, such as cavitation and fuel atomization [1-7]. The outcomes of CFD simulation at conditions up to high pressures are dependent on accurate representation of fluid physical properties. For extreme conditions, limited experimental thermal conductivity data are available for well-characterized hydrocarbon mixtures, and there is a greater lack of thermal conductivity data available for complex mixtures, such as rocket propellant (RP), jet, and diesel fuels. Various correlations and

theories have been developed for the prediction of thermal conductivity for pure hydrocarbons [8-32] and their mixtures [13, 21-23, 30, 33-37] including structure-based group-contribution methods [38-44].

A few pseudo-component based methodologies have been developed to model the thermal conductivity of complex mixtures, such as crude oil and its fractions. These methodologies include an expanded fluid-based (EFB) model [37, 45] and a corresponding-states approach defined by an effective carbon number (ECN) [21]. Yarranton and co-workers [37] used EFB to model the thermal conductivity of several crude oils up to 100 bar and 398 K. They fit four EFB pseudo-component parameters for the crude oils to available experimental data and predicted the thermal conductivity within 1% mean absolute percent deviation (MAPD) compared to experimental data [37]. They extended this work by developing structure independent correlations to calculate the EFB parameters and obtained predictions within 3% MAPD [45]. Teja and Tarlneu [21] used the ECN-based approach to predict the thermal conductivity of different cuts of three crude oils at temperatures from 308 to 528 K and atmospheric pressure within 7% MAPD. Their ECN-based model required as inputs the average molecular weight (MW) and critical properties of the pseudo-components, which were calculated using the reported boiling temperature and specific gravity of the pseudo-components [46] through the correlations developed by Kesler and Lee [47].

The two-abovementioned pseudo-component based techniques capture the effect of composition only through the mixture average MW and are limited in predictive capability by the need for multiple pseudo-components or for fitting to experimental data. Hence, a technique is needed that considers the effects of both the molecular structure and MW of compounds present in mixtures while only requiring a minimum number of parameters fit to experimental data.

In this study, a single pseudo-component technique is developed using the residual entropy scaling based thermal conductivity correlation of Hopp and Gross [26] and the Perturbed-Chain Statistical Associating Fluid Theory (PC-SAFT) [48] equation of state (EoS). Thermal conductivities of well-characterized hydrocarbon mixtures and fuels are predicted up to high temperature and high pressure (HTHP) conditions using two mixture properties: the number averaged MW and hydrogen to carbon (HN/CN) ratio. Less accurate predictions are obtained using the two-parameter model for the mixtures containing high amounts of iso-alkanes, but the predictions are improved when a single thermal conductivity data point at a reference condition is used to fix the value of one model parameter. The technique described here accurately predicts thermal conductivity up to HTHP conditions for fourteen well-characterized hydrocarbon mixtures and six fuels.

Technique Development

PC-SAFT pseudo-component technique

For pure compounds which do not exhibit association, the PC-SAFT EoS of Gross and Sadowski [48] requires three input parameters: m, the number of segments; σ, the segment diameter; and ε/k, the depth of the potential well. The reduced, residual Helmholtz free energy, $\tilde{a}^{\mathrm{res}}$, of a pure compound is then expressed as:

$$\tilde{a}^{\mathrm{res}} = \tilde{a}^{\mathrm{hc}} + \tilde{a}^{\mathrm{disp}} \tag{1}$$

where $\tilde{a}^{\mathrm{hc}}$ and $\tilde{a}^{\mathrm{disp}}$ are the reduced, Helmholtz free energies for the hard-chain reference fluid and dispersion interactions, respectively. Pure compound PC-SAFT parameters are determined by directly fitting to properties (*e.g.*, saturated liquid density and vapor pressure data) or using group contribution (GC) methods [49-51]. In this study, the PC-SAFT parameters are determined using the GC parameters of Sauer et al. [49] to be consistent with our earlier reported technique to predict

viscosity [52]. However, in general, other PC-SAFT GC parameters could be used, such as those reported by Tihic et al. [53] or Burgess et al. [54]. PC-SAFT parameters are fit as a function of molecular weight (MW) for a given chemical family. Table 1 presents the correlations for m, $m\sigma$, and ε/k for n-alkanes and poly-nuclear aromatics (PNAs), which provide numerical bounds for the m, σ, and ε/k values of other chemical families [55].

Equations 2-4 use a Z parameter to average the contributions from the two bounds. Z varies from zero for n-alkanes to one for PNAs, and is used to normalize the degree of unsaturation (DoU), as shown in Eq. 5. Equations 6 and 7 are used to calculate the pseudo-component DoU knowing the mixture number averaged MW and HN/CN ratio. Here we note that phenanthrene (MW = 178 g/mol, DoU = 10) is the largest PNA in the hydrocarbon mixtures and fuels [55]. Hence, the upper bound value for DoU is fixed at 10 in Eq. 5 when the mixture number averaged MW is greater than 178 g/mol. The DoU correlation for PNAs as a function of MW is provided in the Supplemental Information (SI). More details on the calculation of the PC-SAFT pseudo-component parameters can be found in our previous study [55]. A commercial software (VLXE/Blend [56]) is used to calculate the reduced residual entropy, $\tilde{s}^{res}$, shown in Eq. 8, where $\bar{s}^{res}$ is equal to the molar residual entropy divided by the gas constant, R. The next section describes the steps needed for the calculation of the thermal conductivity knowing $\tilde{s}^{res}$.

Table 1. Correlations [52] for PC-SAFT parameters as a function of MW (g/mol) for n-alkanes and PNAs based on the GC parameters of Sauer et al. [49].

	n-alkanes	PNAs
m	$0.0325\text{MW} + 0.2463$	$0.0231\text{MW} + 0.7392$
$m\sigma$ (Å)	$0.1265\text{MW} + 0.7564$	$0.0874\text{MW} + 2.6366$
$\varepsilon/_k$ (K)	$\exp(5.4762 - 1.3302/\text{MW})$	$\exp(5.8137 - 15.5490/\text{MW})$

$$m_{\text{pseudo}-\text{component}} = (1-Z)m_{\text{n}-\text{alkane}} + Zm_{\text{PNA}} \quad (2)$$

$$(m\sigma)_{\text{pseudo}-\text{component}} = (1-Z)(m\sigma)_{\text{n}-\text{alkane}} + Z(m\sigma)_{\text{PNA}} \quad (3)$$

$$\left(\varepsilon/k\right)_{\text{pseudo}-\text{component}} = (1-Z)\left(\varepsilon/k\right)_{\text{n}-\text{alkane}} + Z\left(\varepsilon/k\right)_{\text{PNA}} \quad (4)$$

$$Z = \begin{cases} \dfrac{\text{DoU}_{\text{pseudo}-\text{component}}}{\text{DoU}_{\text{PNA}}}, & \text{MW}_{\text{pseudo}-\text{component}} < 178\ \text{g/mol} \\ \dfrac{\text{DoU}_{\text{pseudo}-\text{component}}}{10}, & \text{MW}_{\text{pseudo}-\text{component}} \geq 178\ \text{g/mol} \end{cases} \quad (5)$$

$$\text{CN} = \frac{\text{MW}_{\text{pseudo}-\text{component}}}{12.01 + 1.01(\text{HN}/\text{CN})_{\text{pseudo}-\text{component}}} \quad (6)$$

$$\text{DoU} = \frac{1}{2}(2 \times \text{CN} + 2 - \text{HN}) \quad (7)$$

$$\tilde{s}^{res}(V,T) = -\left(\frac{\partial \tilde{a}^{\text{res}}}{\partial T}\right)_V \quad (8)$$

Entropy scaling based pseudo-component technique

As observed by Rosenfeld [57], the reduced thermal conductivity, λ^*, (Eq. 9) of a pure compound scales with the residual entropy. Hopp and Gross [26] investigated several choices of a reference thermal conductivity including Chapman Enskog (CE), CE with Eucken correction, and the reference proposed by Liang and Tsai [58] based on the work of Stiel and Thodos [59]. None of these references was completely successful in describing the nonlinear entropy scaling behavior for the complete fluid space from low-density gas to dense liquid. Hopp and Gross [26] proposed a new, empirically-based reference that did correlate the complete fluid space and allowed for a mono-variable dependence on reduced residual entropy. Hopp and Gross [26] showed that the CE reference thermal conductivity (Eq. 10) can adequately reproduce λ^* in the dense fluid region,

which is the region of interest in the present study. Hence, the CE reference term is used as the reference thermal conductivity in the present study.

$$\lambda^* = \frac{\lambda}{\lambda_{\text{reference}}} \tag{9}$$

$$\lambda_{\text{reference}} = \lambda_{\text{CE}} = \frac{5}{16}\frac{\sqrt{\text{MW}kT/\left(mN_{\text{A}}\pi\right)}}{\sigma^2\Omega(2,2)*} \tag{10}$$

where, k, T, N_A, and $\Omega^{(2,2)*}$ are Boltzmann's constant, temperature, Avogadro's number, and the reduced collision integral, respectively. In Eq. 10, m and σ are the PC-SAFT parameters of a pure compound when calculating thermal conductivity for a pure compound or are those of a pseudo-component when calculating thermal conductivity of a pseudo-component. Hopp and Gross [26] modified the third-order polynomial reported by Lötgering-Lin and Gross [60] for viscosity and proposed Eq. 11 to correlate λ^* to the reduced, dimensionless residual, entropy, s^* (Eq. 12).

$$ln(\lambda^*) = A + Bs^* + C(1.0 - \exp(s^*)) + Ds^{*2} \tag{11}$$

$$s^* = \left(\frac{\tilde{s}^{res}(V,T)}{m}\right) \tag{12}$$

where A, B, C, and D are the thermal conductivity coefficients. In the present study, instead of using Eq. 11 to calculate λ^*, the simpler expression in Eq. 13 is used since it adequately describes liquid-phase thermal conductivities.

$$ln(\lambda^*) = A + Bs^* + Cs^{*2} + Ds^{*3} \tag{13}$$

where the thermal conductivity coefficients of a pure compound are used when calculating thermal conductivity of a pure compound or those of a pseudo-component are used when calculating the thermal conductivity of a pseudo-component.

Hopp and Gross [26] used Eq. 11 to fit thermal conductivity coefficients for 148 pure compounds that included normal and iso-alkanes, alkenes, aldehydes, ethers, esters, ketones, alcohols, acids, and benzenes. However, they did not report parameters for some compounds from chemical classes present in petro-fuels including cyclohexanes, decalins, tetralins, indanes, naphthalenes, and phenanthrenes due to the limited amount of thermal conductivity data available in the literature. In the pseudo-component approach, n-alkanes and PNAs are the two bounds for values of the thermal conductivity coefficients. Since Hopp and Gross [26] did not report coefficients for n-alkanes and PNAs using only the CE reference term, new pure compound liquid phase thermal conductivity coefficients (*i.e.*, *A,B,C,D*) are fit in the present study.

For many n-alkanes and PNAs, experimental thermal conductivity data at HTHP conditions are not reported in the literature. Thus, experimental thermal conductivities at atmospheric pressure are utilized here to fit the n-alkane parameters. Experimental data is lacking for PNAs even at atmospheric pressure, with the exception of benzene. Briggs [61] reported a thermal conductivity correlation as a function of temperature at atmospheric pressure for some PNAs (*i.e.*, benzene, naphthalene, and phenanthrene). However, thermal conductivities of benzene using the Briggs correlation deviate by up to 8% compared to data reported in the Dortmund Data Bank (DDB) [62] containing data of Rastorguev and Pugach [63]. Here we use the model of Gharagheizi et al. [38] for benzene at atmospheric pressure to predict thermal conductivity within 4% of the DDB. Furthermore, since no other experimental data for heavier PNAs are available to assess the accuracy of the Briggs correlation [61], the model of Gharagheizi et al. [38] is also used

to calculate the thermal conductivities of naphthalene and phenanthrene (PNAs) at atmospheric pressure. More information on the differences between the thermal conductivities of benzene, naphthalene, and phenanthrene using these two approaches is reported in the SI. Table 2 lists coefficients A, B, C and D fit to Eq. 13 for selected n-alkanes and PNAs. For n-alkanes, A does not vary monotonically with MW. B decreases with MW, whereas C and D appear constant for n-alkanes. For PNAs, A, B, and C monotonically increase with MW, whereas D is a constant. Figure 1 shows these coefficients plotted versus MW for n-alkanes and PNAs, and the correlations are listed in Table 3.

Table 2. Thermal conductivity coefficients fit to atmospheric pressure data using Eq. 13 for selected n-alkanes and PNAs.

Compounds	A	B	C	D	T_{range} / K	λ_{range} / $Wm^{-1}K^{-1}$	Reference
n-octane	0.482	-0.972	-0.001	0.013	298-348	0.127-0.112	Kashiwagi et al. [64]
n-decane	0.482	-0.990	-0.001	0.013	303-373	0.130-0.110	Kashiwagi et al. [64]
n-undecane	0.482	-1.002	-0.001	0.013	292-364	0.135-0.120	Wada et al. [65]
n-dodecane	0.482	-1.008	-0.001	0.013	298-373	0.136-0.119	Kashiwagi et al. [64]
n-tetradecane	0.506	-1.009	-0.001	0.013	284-363	0.143-0.126	Wada et al. [65]
n-hexadecane	0.506	-1.024	-0.001	0.013	296-362	0.144-0.132	Wada et al. [65]
benzene	0.303	-1.362	-0.217	-0.013	279-413	0.145-0.118	Gharagheizi et al. [38]
naphthalene	0.367	-1.307	-0.195	-0.013	354-545	0.126-0.088	Gharagheizi et al. [38]
phenanthrene	0.415	-1.293	-0.183	-0.013	375-483	0.129-0.107	Gharagheizi et al. [38]

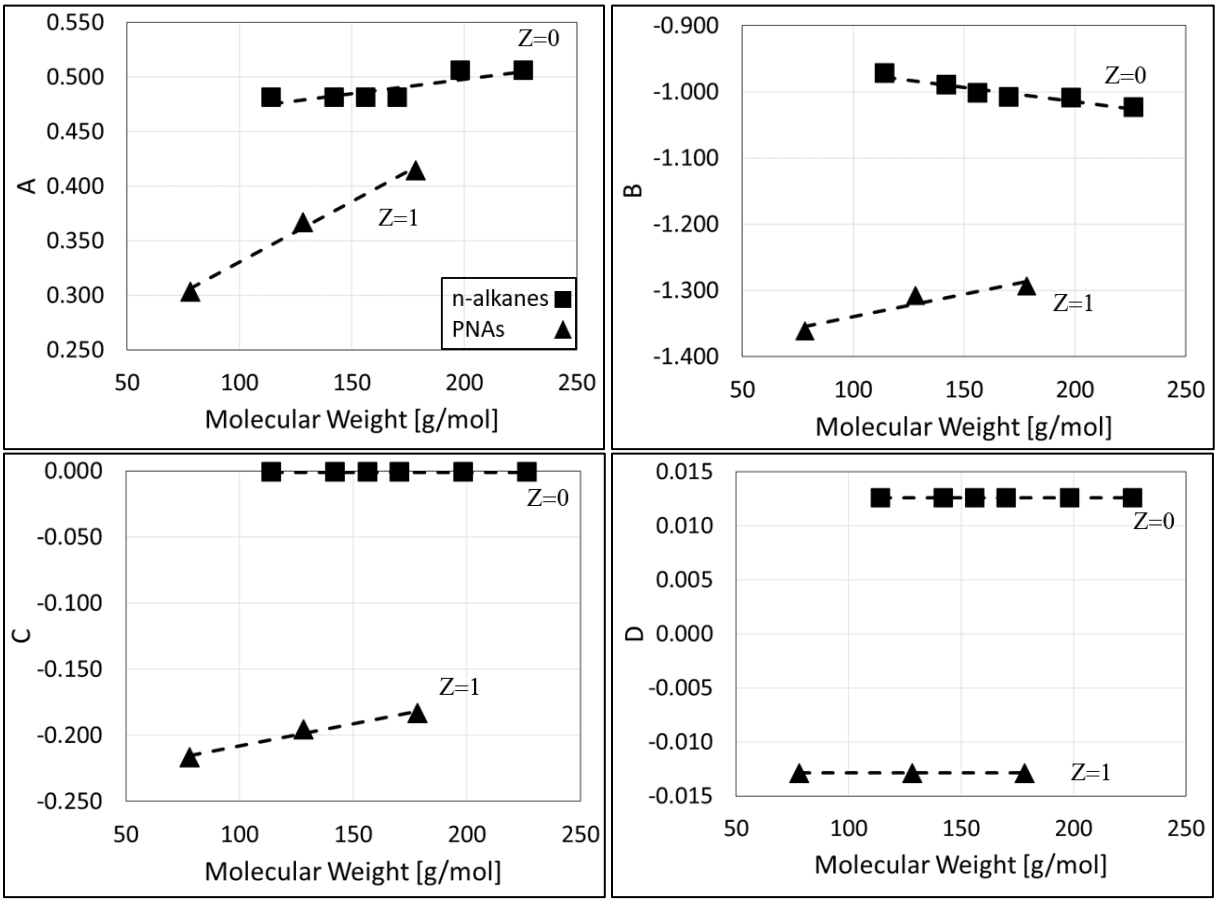

Figure 1. Effect of molecular weight (g/mol) on thermal conductivity coefficients for selected compounds from n-alkanes and PNAs. Note that the y-axis scale is different in each figure.

Table 3. Thermal conductivity coefficient correlations as a function of MW (g/mol) fit to selected compounds from n-alkanes and PNAs.

Coefficient	n-alkanes	PNAs
A	$2.6702 \times 10^{-4}\mathrm{MW} + 4.4472 \times 10^{-1}$	$1.1140 \times 10^{-3}\mathrm{MW} + 2.1893 \times 10^{-1}$
B	$-4.2810 \times 10^{-4}\mathrm{MW} - 9.2891 \times 10^{-1}$	$6.8258 \times 10^{-4}\mathrm{MW} - 1.4083 \times 10^{0}$
C	-1.0012×10^{-3}	$3.3215 \times 10^{-4}\mathrm{MW} - 2.4099 \times 10^{-1}$
D	1.2568×10^{-2}	-1.2867×10^{-2}

In our previous study [52], the viscosity coefficients for chemical classes present in fuel were scaled with PC-SAFT parameter *m*, so that parameter values for n-alkanes and PNAs bounded parameter values for all other chemical families. Due to the lack of thermal conductivity data available in the literature for the pure compounds from different chemical classes found in fuels, only the thermal conductivity coefficients for n-alkanes and PNAs are considered here and the coefficients for the two groups are assumed to be the two bounds for the pseudo-component thermal conductivity coefficients in Eq. 13. The Z value, calculated using Eq. 5, is used in Eqs. 14-17 to calculate the pseudo-component thermal conductivity coefficients needed for the calculation of the reduced thermal conductivity using Eq. 13.

$$A_{\text{pseudo}-\text{component}} = (1-Z)A_{\text{n}-\text{alkane}} + ZA_{\text{PNA}} \tag{14}$$

$$B_{\text{pseudo}-\text{component}} = (1-Z)B_{\text{n}-\text{alkane}} + ZB_{\text{PNA}} \tag{15}$$

$$C_{\text{pseudo}-\text{component}} = (1-Z)C_{\text{n}-\text{alkane}} + ZC_{\text{PNA}} \tag{16}$$

$$D_{\text{pseudo}-\text{component}} = (1-Z)D_{\text{n}-\text{alkane}} + ZD_{\text{PNA}} \tag{17}$$

When applying this approach to well-characterized hydrocarbon mixtures and fuels, thermal conductivity predictions improve by fitting B to a single reference state data point. In this study, the reference state is chosen as the experimental data point at the lowest reported temperature and pressure for the samples of interest. Coefficient B is fit to reproduce the thermal conductivity at the reference state, while A, C, and D are determined from Eqs. 14, 16, and 17. The results for the two-parameter and three-parameter models are described in the following sections for well-characterized hydrocarbon mixtures and fuels.

The thermal conductivity predictions are compared with 655 data points for well-characterized hydrocarbon mixtures, rocket propellant fuels, and jet fuels. The performance of our approach is characterized by the percent deviation, maximum (Max) deviation, standard deviation (SD), MAPD, and bias, in Eqs. 18-22.

$$Deviation\ (\%) = 100 \times \frac{\left(\lambda_{\text{predict}} - \lambda_{\text{exp}}\right)}{\lambda_{\text{exp}}} \tag{18}$$

$$Max\ Deviation\ (\%) = Max\ (100 \times \frac{\left|\lambda_{\text{predict}} - \lambda_{\text{exp}}\right|}{\lambda_{\text{exp}}}) \tag{19}$$

$$SD\ (\%) = \sqrt{\frac{\sum\left(\lambda - \bar{\lambda}\right)^2}{N-1}} \tag{20}$$

$$MAPD\ (\%) = \frac{1}{N}\sum 100 \times \frac{\left|\lambda_{\text{predict}} - \lambda_{\text{exp}}\right|}{\lambda_{\text{exp}}} \tag{21}$$

$$Bias\ (\%) = \frac{1}{N}\sum 100 \times \frac{\left(\lambda_{\text{predict}} - \lambda_{\text{exp}}\right)}{\lambda_{\text{exp}}} \tag{22}$$

where, λ_{predict}, λ_{exp}, $\bar{\lambda}$, and N are the experimental thermal conductivity, the predicted thermal conductivity, the mean of the thermal conductivity, and the number of data points, respectively.

Well-characterized hydrocarbon mixtures

The pseudo-component technique is applied to several binary and ternary hydrocarbon mixtures [65-67]. Wakeham et al. [66] measured the thermal conductivity for binary mixtures containing benzene and tri-methyl-pentane (TMP) (referred to as M1) for two different compositions at temperatures from 313 to 345 K and pressures up to 3,500 bar. Fareleira et al. [67] and Wakeham et al. [66] reported thermal conductivity data for binary mixtures containing n-heptane (C7) and TMP (referred to as M2) for three different compositions at temperatures from 308 to 360 K and pressures up to 4,500 bar. Wada et al. [65] reported the thermal conductivity data for binary mixtures containing C7 and n-undecane (C11), C7 and n-hexadecane (C16), and

C11 and C16 (referred to as M3, M4, and M5, respectively) for three different compositions for each mixture at atmospheric pressure and a range of temperatures from 295 to 345 K. Wada et al. [65] also reported the thermal conductivity for ternary mixtures (referred to as M6) including C7, C11, and C16 for three compositions at temperatures from 295 to 345 K and 1 bar. Table 4 lists the molar composition of these mixtures. For brevity, only central compositions of mixtures M3-M6 (referred to as M3-2, M4-2, M5-2, and M6-2, respectively) are shown in the figures. However, all mixture compositions of mixtures M3-M6 are included in the reported statistical metrics.

Table 4. Molar composition (mol%) of the well-characterized hydrocarbon mixtures studied in this work. Data from ref. [65-67]

Compound	Chemical Family	M1	M2[a]	M3	M4	M5	M6
n-heptane	n-alkanes	-	48.9 74.4 75.1	25.0 50.0 75.0	-	25.0 50.0 75.0	10.0 33.4 59.9
n-undecane	n-alkanes	-	-	balance	25.0 50.0 75.0	-	29.9 33.3 30.0
n-hexadecane	n-alkanes	-	-	-	balance	balance	balance
tri-methyl-pentane (TMP)	iso-alkanes	25.0 75.0	balance	-	-	-	-
benzene	benzenes	balance	-	-	-	-	-

[a] The composition of mixture M2 containing 74.4 mol% C7 and 25.6 mol% TMP measured by Fareleira et al. [67] is close to that of the mixture containing 75.1 mol% C7 and 24.9 mol% TMP measured by Wakeham et al. [66], and the two data sets agree within 0.05%. Both sets of data are included in the reported statistics in Table 5, but only the data reported by Wakeham et al. [66], which have a greater temperature range, are shown in Figures 2 and 4.

Figures 2 and 3 present the thermal conductivity predictions for the investigated hydrocarbon mixtures at different temperatures and pressures. Figures 4 and 5 show the thermal conductivity prediction deviations for these mixtures. The SI provides information on the calculated MW, HN/CN ratio, Z parameter, thermal conductivity experimental data point (λ_O) at the lowest reported temperature and pressure used to fit B in the three parameter model, the PC-SAFT parameters, and the thermal conductivity coefficients for the pseudo-components for all of the well-characterized hydrocarbon mixtures considered in this study. Table 5 summarizes the statistical metrics of the thermal conductivity predictions for these mixtures.

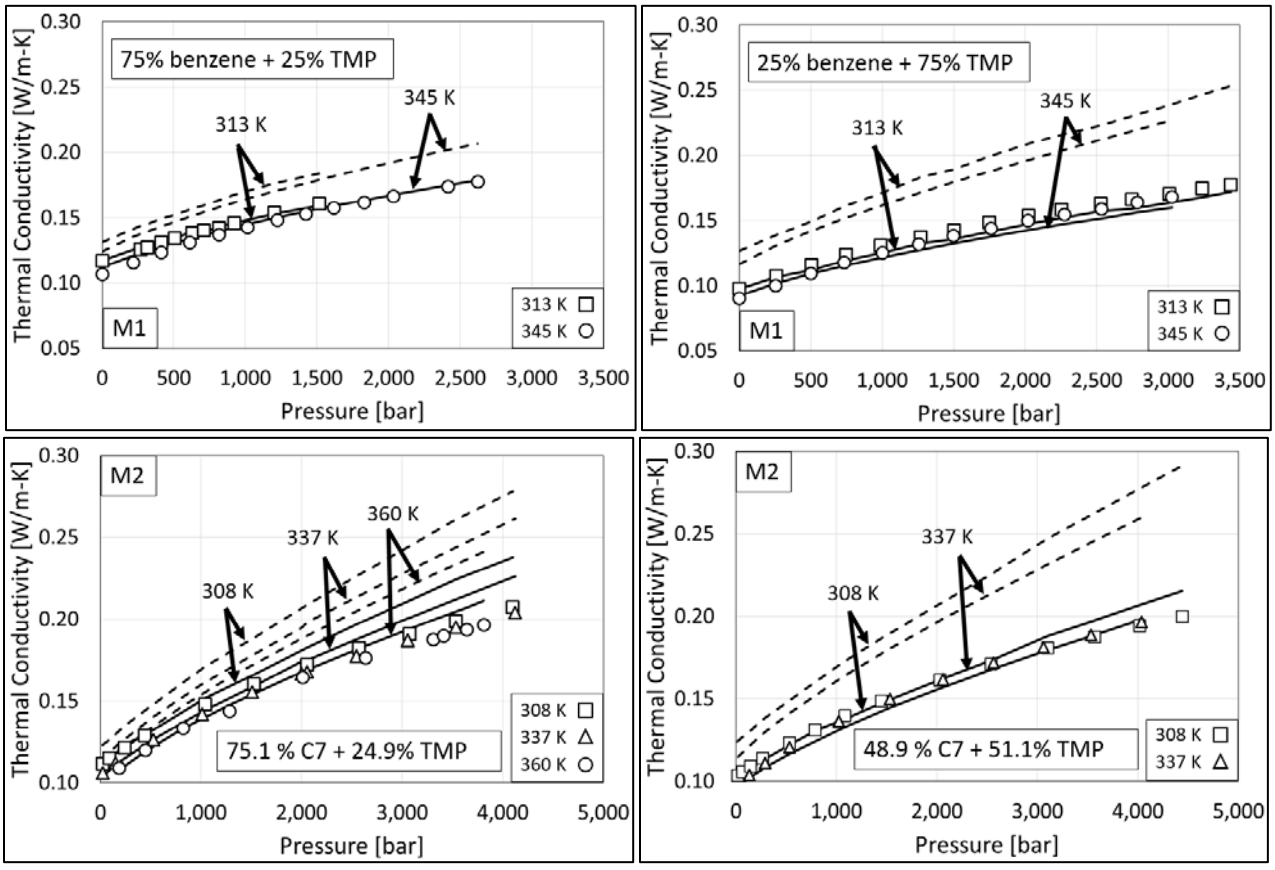

Figure 2. Pseudo-component thermal conductivity predictions compared to experimental data [66, 67] (symbols) for mixtures M1 and M2. Dashed lines show the two-parameter calculations and solid lines show the three-parameter calculations.

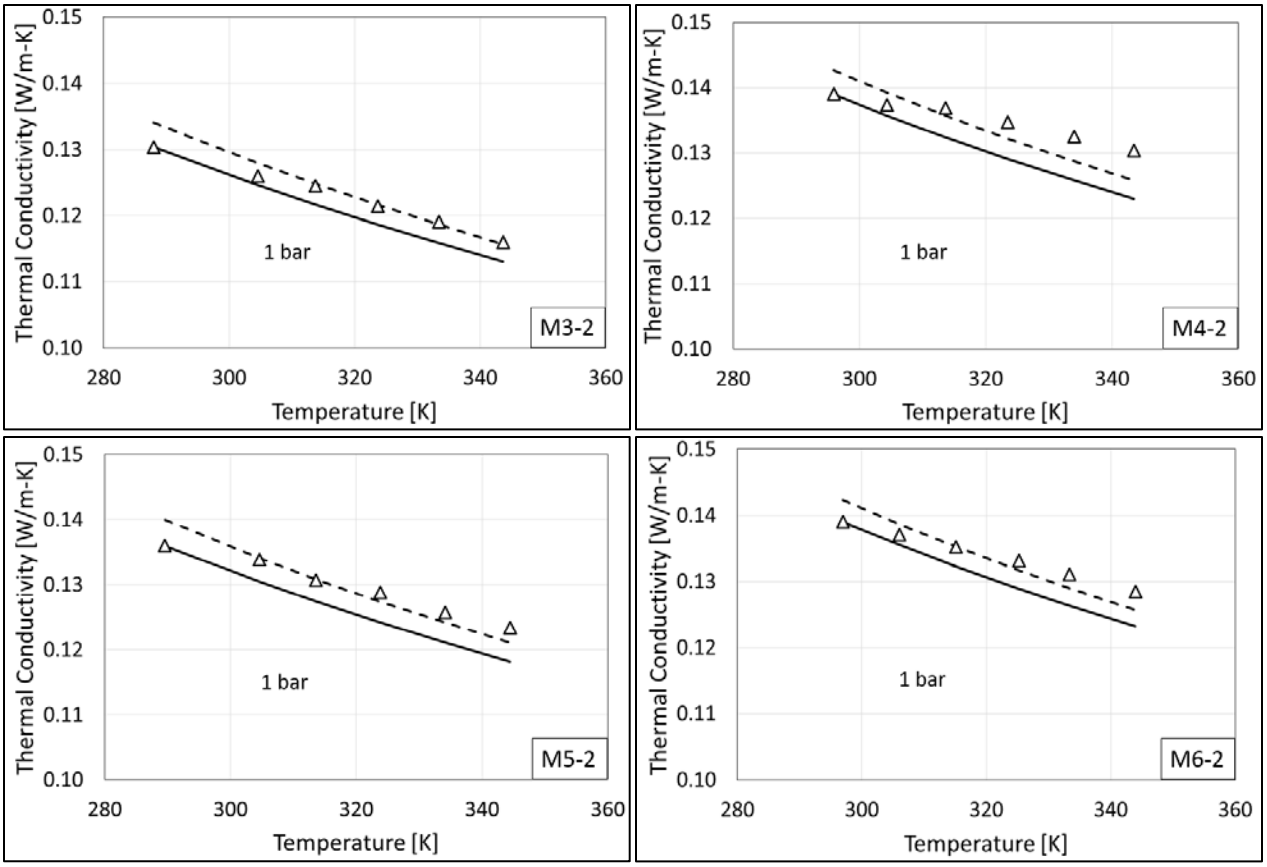

Figure 3. Pseudo-component thermal conductivity predictions compared to experimental data [65] (symbols) for mixtures M3-2 to M6-2. Dashed lines show the two-parameter calculations and solid lines show the three-parameter calculations.

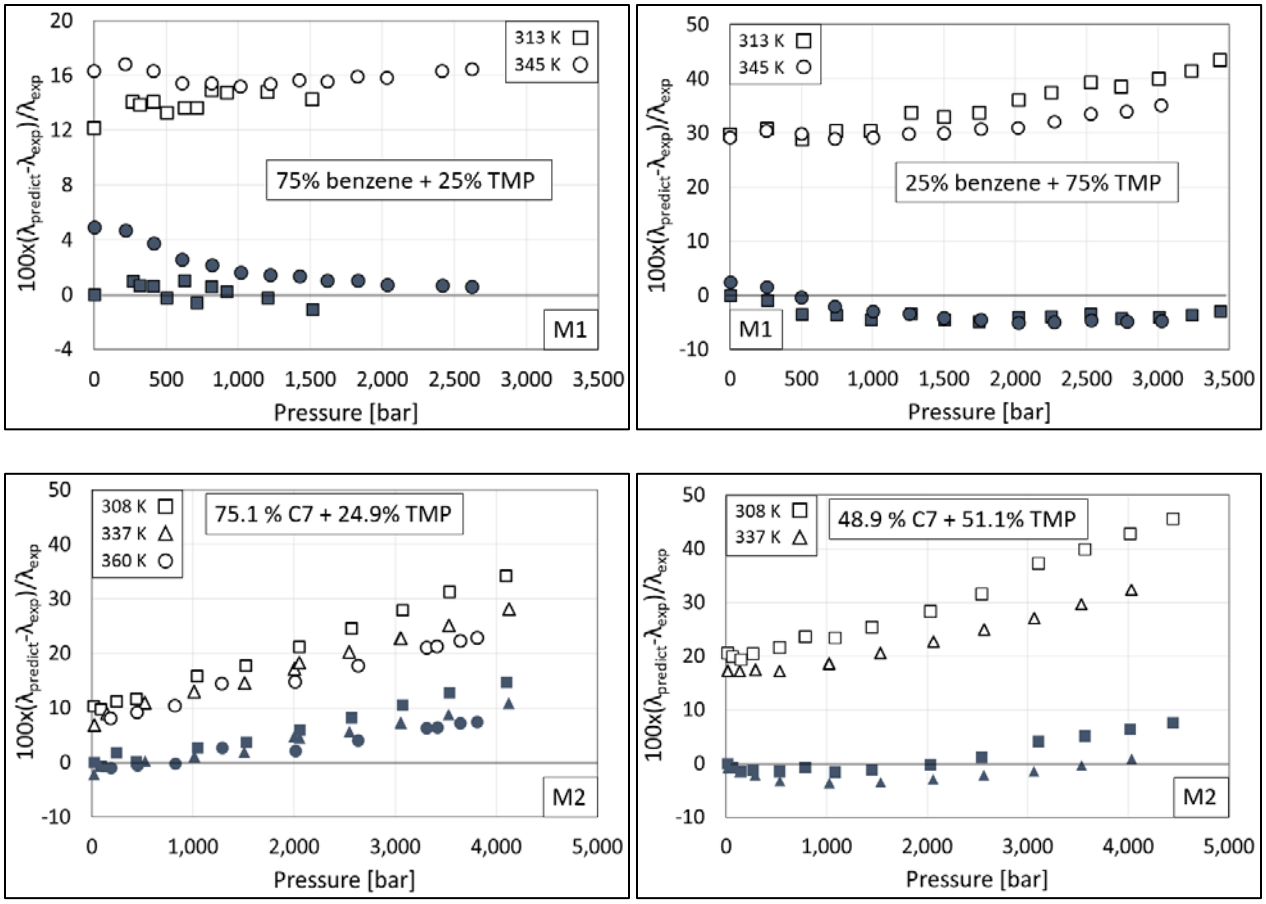

Figure 4. Pseudo-component thermal conductivity prediction deviations compared to experimental data [66, 67] for mixtures M1 and M2: two-parameter (open symbols) and three-parameter (filled symbols) models.

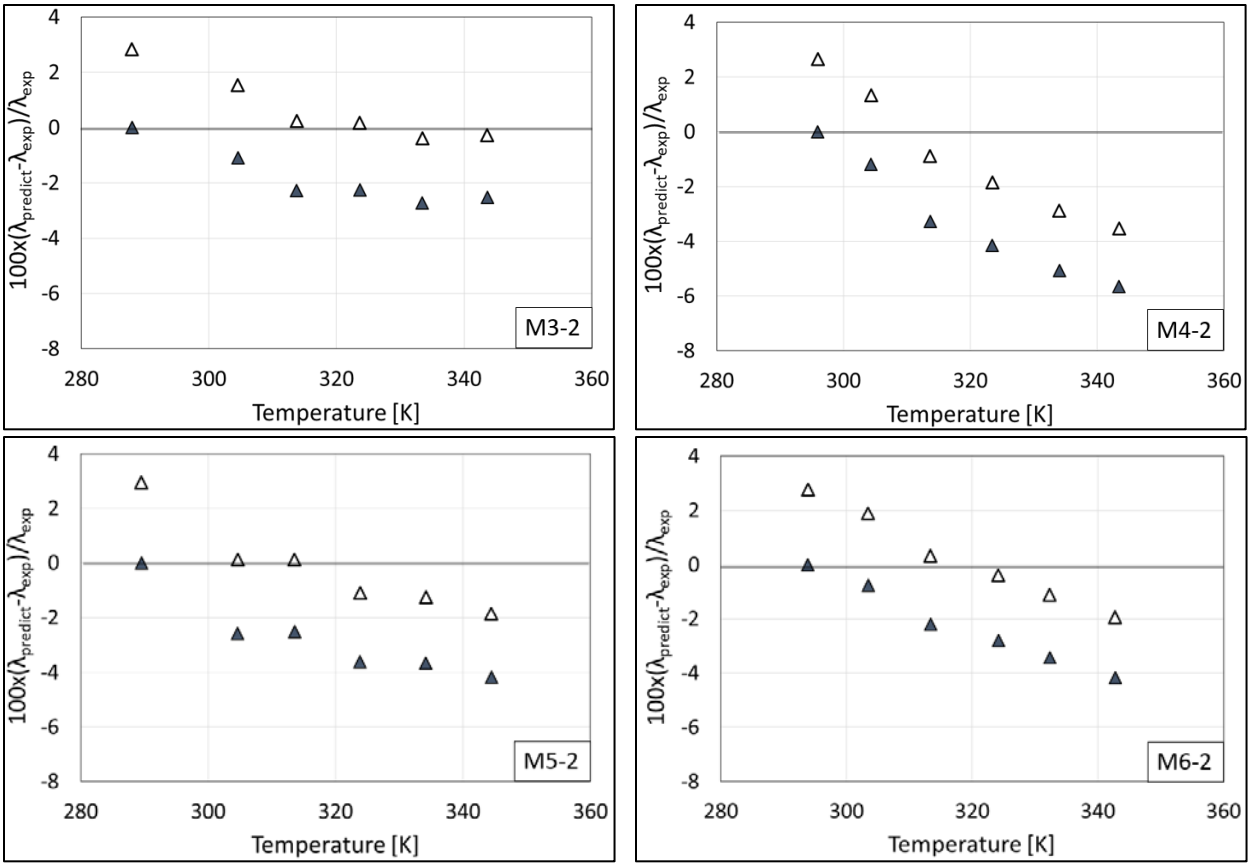

Figure 5. Pseudo-component thermal conductivity prediction deviations compared to experimental data [65-67] for mixtures M3-2 to M6-2 at 1 bar: two-parameter (open symbols) and three-parameter (filled symbols) models.

Table 5. The MAPD (%), bias (%), SD (%), and Max D (%) for the pseudo-component thermal conductivity of well-characterized hydrocarbon mixtures compared to the literature [65-67].

	Two-parameter				Three-parameter			
	MAPD	Bias	SD	Max Deviation	MAPD	Bias	SD	Max Deviation
M1	20.0	20.0	7.9	45.6	3.7	2.6	3.7	15.2
M2	24.6	24.6	9.8	43.4	2.4	-1.3	1.7	5.1
M3	1.2	0.5	0.9	2.8	1.9	-1.9	1.3	4.1
M4	2.0	-0.8	1.0	3.5	2.9	-2.9	2.0	5.6
M5	1.3	0.1	0.9	2.9	2.3	-2.3	1.4	4.2
M6	1.3	0.2	0.9	2.8	2.2	-2.2	1.4	4.2

The pseudo-component technique developed in this study captures the effects of temperature and pressure for all samples. Pseudo-component thermal conductivities are predicted for mixtures M1 and M2 with MAPDs of 20 and 25%, respectively, using the two-parameter model. The MAPDs for thermal conductivity predictions for all compositions of mixtures M1 and M2, shown in the SI, increase as the concentration of TMP, an iso-alkane, increases. More accurate thermal conductivities with MAPDs less than 2% are predicted at atmospheric pressure and a range of temperatures using the two-parameter model for mixtures M3-M6, composed of only n-alkanes. Their better predictions could be due the fact that the correlations in the technique were fit to ambient pressure data. Furthermore, since $Z = 0$ for n-alkane mixtures, the thermal conductivity coefficients in Eqs. 14-17 reduce to the correlations for n-alkanes, leading to reduced error, as there is no mixing with the PNA correlations.

It should be noted that the compounds present in mixtures M1 and M2 (C7 with MW = 100.21 g/mol, benzene with MW = 78.11 g/mol, and TMP with MW = 114.23 g/mol) are at the extreme lower MW bounds of the fitted PC-SAFT parameter and thermal conductivity coefficient correlations. The two-parameter pseudo-component model may not accurately represent the PC-SAFT parameters and thermal conductivity coefficients for mixtures with such low MW compounds. Note that the definition of DoU (Eq. 7) does not distinguish between normal and iso-alkanes, which could be an additional reason for thermal conductivity prediction deviations for mixtures containing significant amounts of iso-alkanes. Inclusion of a single thermal conductivity data point at a chosen reference state to fit *B* improves the predictions for mixtures M1 and M2 containing large amounts of iso-alkanes. Thermal conductivity is predicted for hydrocarbon mixtures using the three-parameter model with an MAPD of 3.0% for all compositions of all

investigated mixtures. This MAPD is comparable to thermal conductivity predictions for all 148 pure compounds studied by Hopp and Gross [26], who reported a 4.2% MAPD.

Fuels

Gasoline, kerosene, jet, and diesel fuel fractions distilled from crude oil are complex mixtures of hydrocarbon compounds with properties and composition that vary due to quality specifications [68, 69]. Table 6 lists the limited HTHP thermal conductivity literature data found only for rocket propellant (RP) and jet fuels. Akhmedova-Azizova et al. [70] measured the thermal conductivity of RP1 fuel at temperatures between 293 and 598 K and pressures up to 600 bar. Bruno [71] measured the thermal conductivity of RP2 fuel over a wide range of temperatures from 300 to 550 K and pressures up to 600 bar. Xu et al. [72] reported thermal conductivity measurements of RP3 fuel at temperatures from 285 to 513 K and pressures up to 50 bar. Jia et al. [73] reported thermal conductivity of RP3 fuel at temperatures from 311 to 399 K and a single isobar at 30 bar. Bruno [74] also measured the thermal conductivity of three different jet fuels including S-8 4734 (referred to as S-8), JP-8 3773 (referred to as JP-8), and Jet A 4658 (referred to as Jet A) at high temperatures from 270 to 470 K and pressures up to 400 bar. Table 7 lists the calculated MW, HN/CN ratio, Z parameter, thermal conductivity reference experimental data point (λ_o) at the lowest reported temperature and pressure used to fit B in the three parameter model, the PC-SAFT parameters, and the thermal conductivity coefficients for the pseudo-components for the fuels.

Table 6. Summary of HTHP thermal conductivity data available in the literature for rocket propellant (RP) and jet fuels.

Reference	Fuel	T_{range}/K	P_{max}/bar	Uncertainty (%)
Akhmedova-Azizova et al. [70]	RP1 [a]	293-598	600	2
Bruno [71]	RP2 [b]	300-550	600	-
Xu et al. [72], Jia et al. [73]	RP3 [c]	285-513	50	3
Bruno [74]	S-8 [d]	304-504	700	3
Bruno [74]	JP-8 [d]	303-407	600	3
Bruno [74]	Jet A [d]	303-501	400	3

[a] The number averaged MW and the HN/CN ratio of the sample are calculated from the molecular formula of a typical RP1 fuel reported by Edwards [75].

[b] The number averaged MW and the HN/CN ratio of the sample are calculated from the molecular formula of a typical RP2 fuel reported by Xu et al. [76].

[c] The number averaged MW and the HN/CN ratio of the sample are calculated from the detailed composition of the RP3 fuel reported by Deng et al. [77]. The 30 bar thermal conductivities reported by Xu et al. [72], which are measured using a double transient hot-wire method, are on average 9% different compared to data reported by Jia et al. [73] at the single pressure of 30 bar, which are measured using a steady and kinetic method, an experimental technique proposed in the article [73]. We note that all three studies [72, 73, 77] are from the same research group.

[d] The number averaged MW and the HN/CN ratio of the samples are reported by Won et al. [78] and Chickos and Zhao [79].

Table 7. The pseudo-component properties and parameters for fuels modeled in this study [70-74]. λ_0 (W/m-K) is the thermal conductivity at the lowest reported temperature and pressure used to fit B, here termed B^{fit}, in the three-parameter model. The lowest temperatures and pressures for the fuels are: RP1 at 293 K and 1 bar, RP2 at 300 K and 2 bar, RP3 at 299 K and 1 bar, S-8 at 304 K and 3 bar, JP-8 at 303 K and 8 bar, and Jet A at 302 K and 2 bar.

Fuel	MW	HN/CN	Z	λ_0	m	σ (Å)	ε/k (K)	A	B	C	D	B^{fit}
RP1	167.7	1.95	0.139	0.113	5.546	3.844	246.5	0.478	-1.041	-0.027	0.009	-0.926
RP2	177.0	2.03	0.082	0.108	5.903	3.851	242.8	0.486	-1.028	-0.016	0.010	-0.893
RP3	153.0	1.93	0.163	0.126	5.065	3.839	247.6	0.470	-1.045	-0.032	0.008	-0.989
JP-8	160.0	1.95	0.144	0.116	5.300	3.842	246.6	0.474	-1.041	-0.028	0.009	-0.948
S-8	154.5	2.14	0.028	0.117	5.241	3.851	238.7	0.483	-1.004	-0.006	0.012	-0.934
Jet A	157.5	1.96	0.140	0.112	5.227	3.842	246.2	0.474	-1.039	-0.027	0.009	-0.933

Figures 6 and 7 present the thermal conductivity predictions for the RP and jet fuels at different temperatures and pressures, respectively. Figures 8 and 9 show the thermal conductivity prediction deviations for these fuels. Table 8 summarizes the statistical metrics of the thermal conductivity predictions for the six fuels. The pseudo-component technique captures the effects of both temperature and pressure on thermal conductivity with an MAPD of 14.3% using the two-parameter model across all temperatures and pressures for all fuels. Two sets of experimental data are reported in the literature for the thermal conductivity of RP3 at 30 bar [72, 73]. Using the two-parameter model, thermal conductivity is predicted with 1% MAPD compared to the data reported by Jia et al. [73] and 9% MAPD compared to data reported by Xu et al. [72]. There is a 9% difference between these two sets of experimental measurements, which were obtained using two different techniques (double transient hot wire and steady and kinetic methods). It should be noted that Jia et al. [73] proposed the steady and kinetic method in the same article as the RP3

measurements at 30 bar. Typical RP and jet fuels contain between 10 to 40 weight percent iso-alkanes [75, 76, 80-82] and also contain amounts of alkylated compounds [72, 76, 81, 82] including alkylated cyclohexanes and alkylated benzenes. The pseudo-component technique does not distinguish the differences between normal and iso-alkanes. Since $Z = 0$ for both normal and iso-alkanes, the effect of the iso-alkanes and alkylated compounds (branching) in the fuel on the thermal conductivity may not be accurately captured using the two-parameter pseudo-component model for the fuels investigated in this study. By including a single thermal conductivity data point as a third input, predictions are significantly improved with an MAPD of 2.0%, which is within the experimental uncertainty of 3% reported in the literature [70-74]. RP3 thermal conductivities at 30 bar are predicted less accurately using the three-parameter model when comparing to the Jia et al. [73] data (8.3 % MAPD) than the Xu et al. [72] data (2.3 % MAPD) .

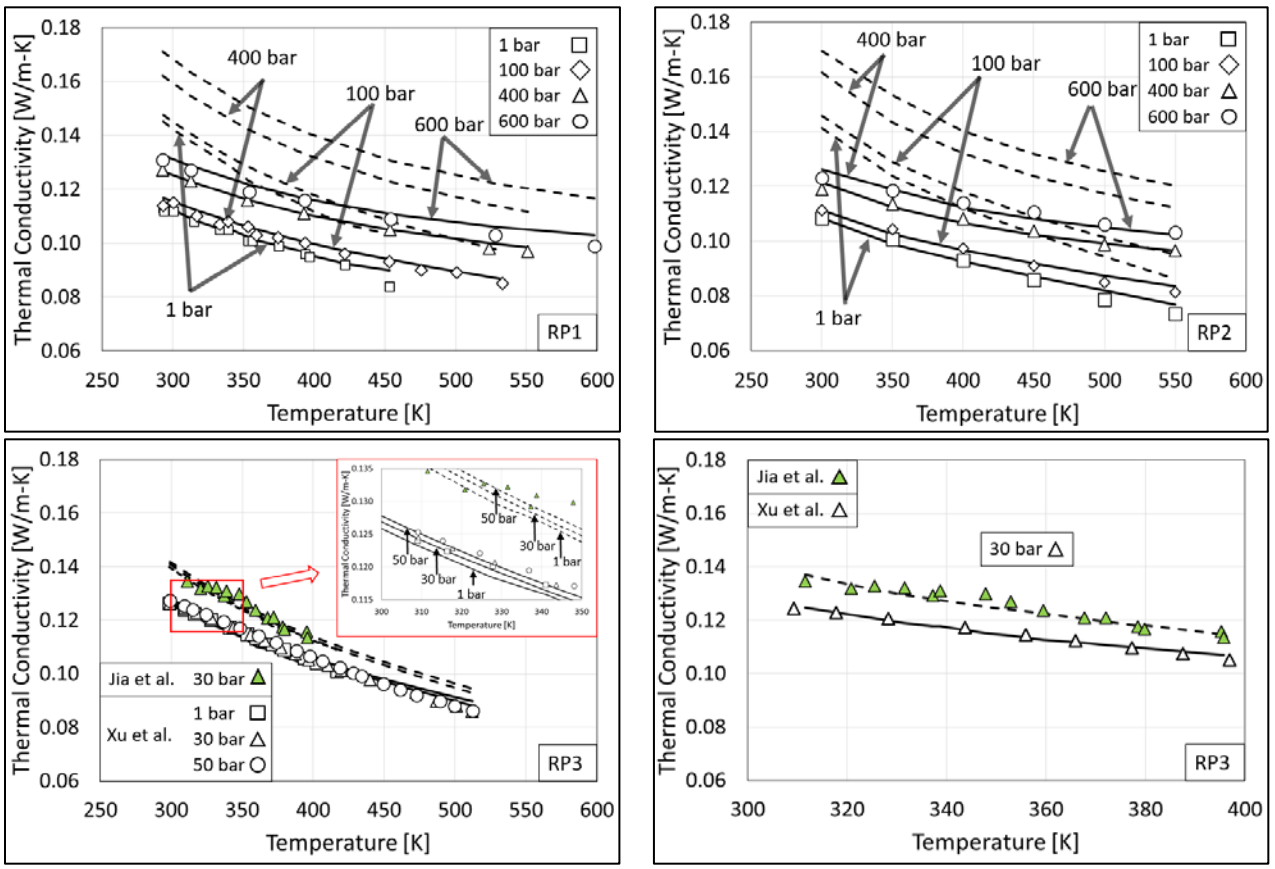

Figure 6. Pseudo-component thermal conductivity predictions compared to experimental data [70-73] (symbols) for rocket propellant (RP) fuels listed in Table 7. Dashed lines show the two-parameter calculations, and solid lines show the three-parameter calculations. A separate figure is shown for the RP3 thermal conductivities at 30 bar, since two data sets [72, 73] were reported in the literature. Note that the x-axis scale is different in the figure for RP3 at 30 bar.

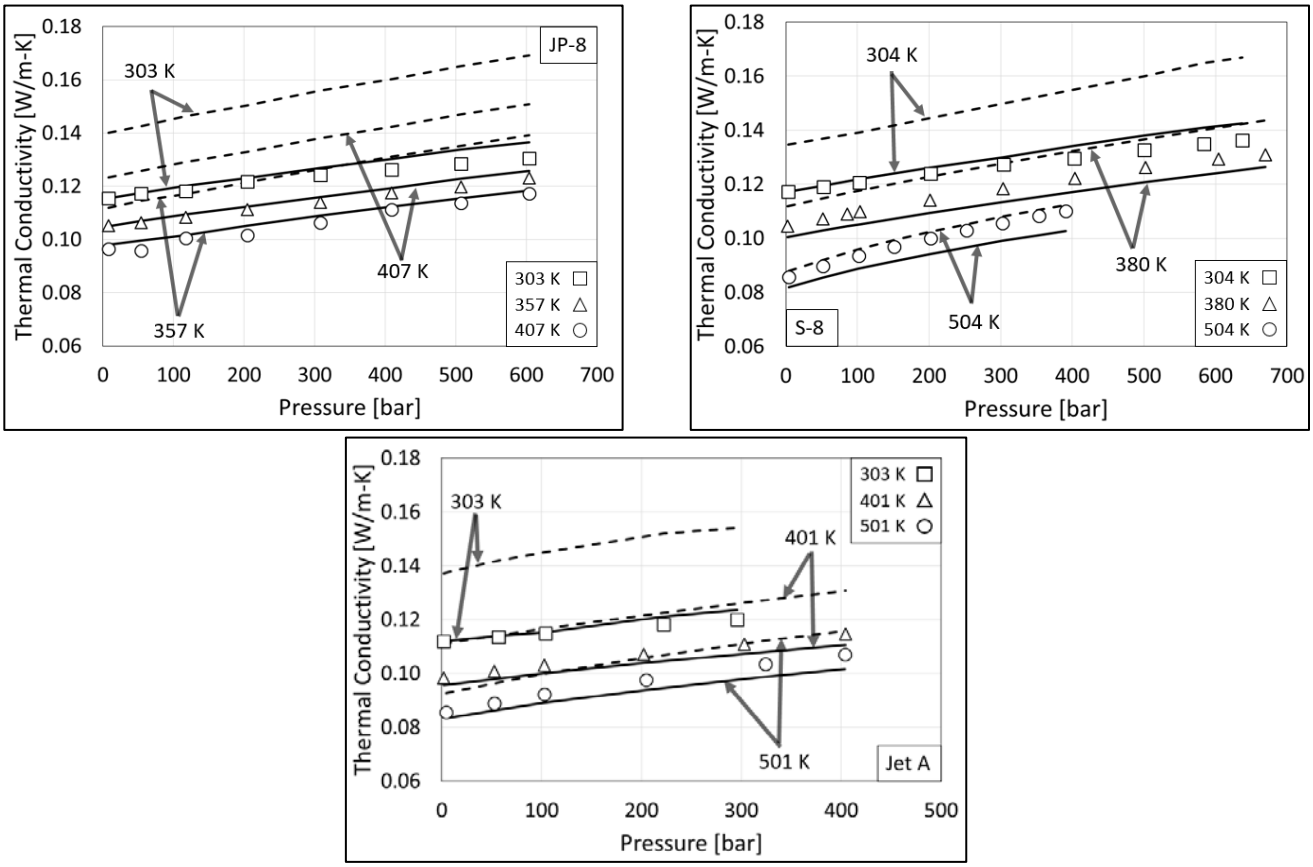

Figure 7. Pseudo-component thermal conductivity predictions compared to experimental data [74] (symbols) for jet fuels listed in Table 7. Dashed lines show the two-parameter calculations, and solid lines show the three-parameter calculations. Note that the x-axis scale is different in the figure for Jet A.

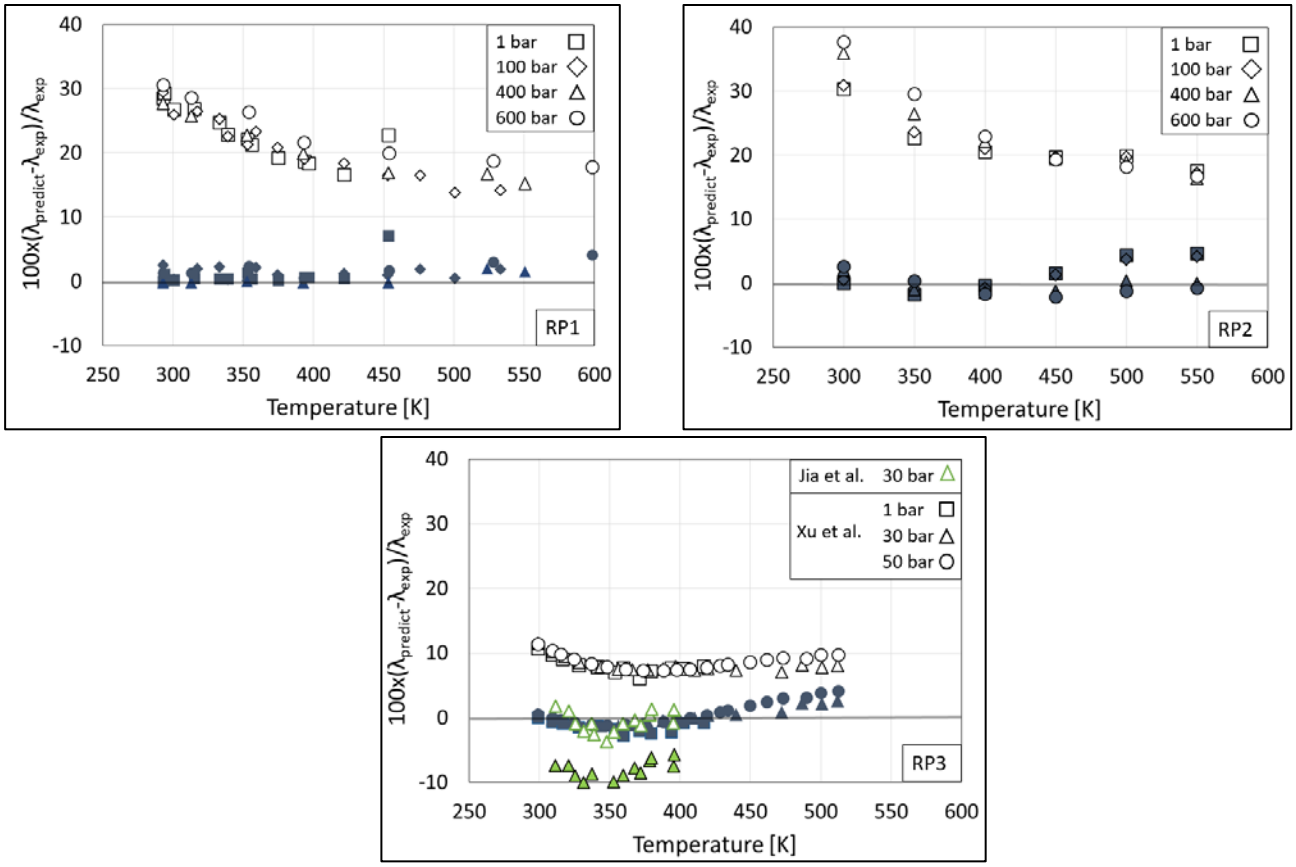

Figure 8. Pseudo-component thermal conductivity predictions deviations compared to experimental data [70-73] for rocket propellant (RP) fuels listed in Table 7: two-parameter (open symbols) and three-parameter (filled symbols) models.

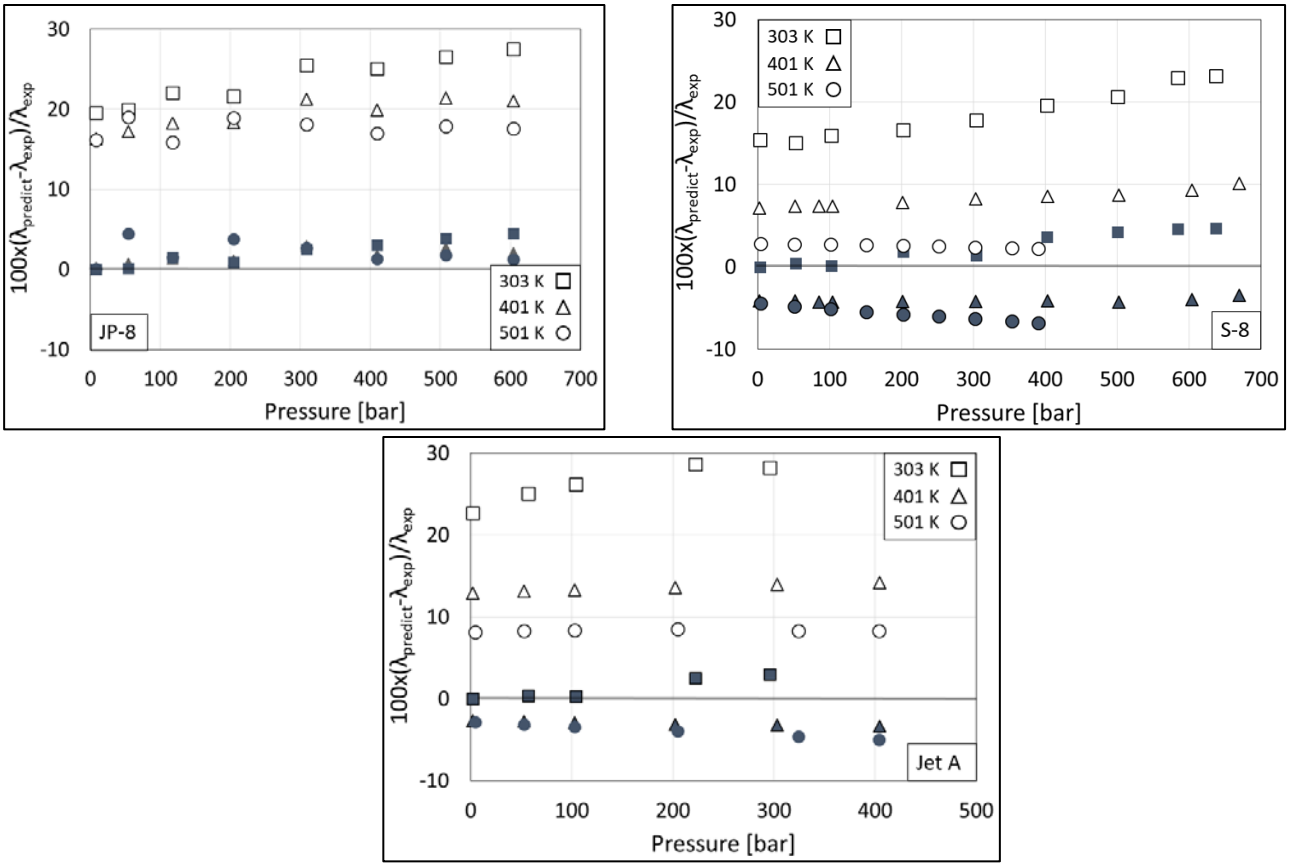

Figure 9. Pseudo-component thermal conductivity predictions deviations compared to experimental data [74] for jet fuels listed in Table 7: two-parameter (open symbols) and three-parameter (filled symbols) models. Note that the x-axis scale is different in the figure for Jet A.

Table 8. The MAPD (%), bias (%), SD (%), and Max D (%) for pseudo-component thermal conductivity predictions of rocket propellant (RP) and jet fuels listed in Table 7 [70-74] at temperatures from 293 to 598 K and pressures up to 700 bar.

	Two-parameter				Three-parameter			
	MAPD	Bias	SD	Max Deviation	MAPD	Bias	SD	Max Deviation
RP1	22.3	22.3	5.4	33.8	1.1	0.5	1.2	6.2
RP2	23.6	23.6	6.7	40.1	1.4	0.0	0.9	3.5
RP3	7.3	7.0	3.5	11.6	2.3	-1.2	2.8	11.2
S-8	13.3	13.3	4.1	22.5	2.2	-0.9	1.4	4.6
JP-8	21.2	21.2	3.6	29.7	1.8	1.8	1.3	4.7
Jet A	15.4	15.4	5.9	30.3	3.1	-2.8	1.5	5.6

Conclusion

A PC-SAFT, pseudo-component technique based on entropy scaling was presented to predict the thermal conductivity of well-characterized hydrocarbon mixtures, rocket propellant fuels, and jet fuels up to high temperature and high pressure (HTHP) conditions. The two experimental mixture properties required to predict thermal conductivity were the number average molecular weight and the hydrogen-to-carbon ratio. Correlations for the model parameters were developed from pure component thermal conductivity coefficients fit at atmospheric pressure. However, the predicted thermal conductivities deviated from the experimental data for mixtures containing significant amounts of iso-alkanes. A third input, the thermal conductivity at a single low-temperature, low-pressure reference state was incorporated in the model to improve the predictions for the mixtures of interest. Although the model was developed from atmospheric pressure data, accurate predictions were obtained when the technique was applied to well-characterized hydrocarbon mixtures and fuels up to HTHP conditions. The method was predictive

and did not require measurement of or fitting to HTHP thermal conductivity data. Thermal conductivities were predicted for fuels at conditions from 285 to 598 K and up to 700 bar using the three-parameter pseudo-component technique with a mean absolute percent deviation of 2.0%, which is within 3%, the reported uncertainty of the experimental measurements.

Acknowledgments

This project has received funding from the European Union Horizon 2020 Research and Innovation program, Grant Agreement No 675528. The authors wish to thank Joseph Roos (Afton), Joseph Remias (Afton), Mark Devlin (Afton), Madlen Hopp (University of Stuttgart), and Joachim Gross (University of Stuttgart) for their helpful, technical discussions.

Nomenclature

English symbols

$\tilde{a}$	reduced Helmholtz free energy
Å	Angstrom
A, *B*, *C*, and *D*	thermal conductivity coefficients
CN	carbon number
HN	hydrogen number
k	Boltzmann constant
K	Kelvin
m	number of segments
N	number of data points
N_A	Avogadro's number
$\bar{s}$	molar entropy
$\tilde{s}$	reduced entropy
s^*	reduced dimensionless residual entropy
T	temperature
V	volume
X	mole fraction
Z	averaging parameter, Eq. 5

Greek symbols

σ	segment diameter
$\Omega^{(2,2)*}$	reduced collision integral
ε/k	depth of the potential well

λ	thermal conductivity
λ_o	thermal conductivity experimental data at the lowest reported temperature and pressure
λ	thermal conductivity
λ^*	reduced thermal conductivity
$\bar{\lambda}$	thermal conductivity mean

Superscripts/Subscripts

CE	Chapman-Enskog
disp	dispersion
exp	experimental data
hc	hard-chain
predict	prediction
res	residual

References

[1] Arcoumanis C, Gavaises M. Linking nozzle flow with spray characteristics in a diesel fuel injection system. Atomization and Sprays **1998**;8(3):307-47.

[2] Battistoni M, Grimaldi CN. Numerical analysis of injector flow and spray characteristics from diesel injectors using fossil and biodiesel fuels. Applied Energy **2012**;97:656-66.

[3] Giannadakis E, Gavaises M, Arcoumanis C. Modelling of cavitation in diesel injector nozzles. Journal of Fluid Mechanics **2008**;616:153-93.

[4] Park SH, Suh HK, Lee CS. Effect of cavitating flow on the flow and fuel atomization characteristics of biodiesel and diesel fuels. Energy & Fuels **2008**;22(1):605-13.

[5] Pomraning E, Richards K, Senecal PK. Modeling turbulent combustion using a RANS model, detailed chemistry, and adaptive mesh refinement. *SAE Technical Paper*. 2014-01-1116. **2014**.

[6] Schmidt DP, Corradini ML. The internal flow of diesel fuel injector nozzles: A review. International Journal of Engine Research **2001**;2(1):1-22.

[7] Senecal PK, Pomraning E, Richards K, Som S. Grid convergent spray models for internal combustion engine CFD simulations. ASME 2012 Internal Combustion Engine Division Fall Technical Conference **2012**(55096):697-710.

[8] Baroncini C, di Filippo P, Latini G, Pacetti M. An improved correlation for the calculation of liquid thermal conductivity. International Journal of Thermophysics **1980**;1(2):159-75.
[9] Baroncini C, di Filippo P, Latini G, Pacetti M. Organic liquid thermal conductivity: A prediction method in the reduced temperature range 0.3 to 0.8. International Journal of Thermophysics **1981**;2(1):21-38.
[10] Baroncini C, di Filippo P, Latini G. Thermal conductivity estimation of the organic and inorganic refrigerants in the saturated liquid state. International Journal of Refrigeration **1983**;6(1):60-2.
[11] Latini G. Thermophysical properties of fluids: dynamic viscosity and thermal conductivity. Journal of Physics: Conference Series **2017**;923-012001:1-12.
[12] Latini G, di Nicola G, Pierantozzi M. Liquid thermal conductivity prediction for alkanes, ketones and silanes. Physics and Chemistry of Liquids **2017**;55(6):747-65.
[13] Baroncini C, Latini G, Pierpaoli P. Thermal conductivity of organic liquid binary mixtures: measurements and prediction method. International Journal of Thermophysics **1984**;5(4):387-401.
[14] Sastri SRS, Rao KK. A new temperature–thermal conductivity relationship for predicting saturated liquid thermal conductivity. Chemical Engineering Journal **1999**;74(3):161-9.
[15] Chung TH, Ajlan M, Lee LL, Starling KE. Generalized multiparameter correlation for nonpolar and polar fluid transport properties. Industrial & Engineering Chemistry Research **1988**;27(4):671-9.
[16] Chung TH, Lee LL, Starling KE. Applications of kinetic gas theories and multiparameter correlation for prediction of dilute gas viscosity and thermal conductivity. Industrial & Engineering Chemistry Fundamentals **1984**;23(1):8-13.
[17] Huber ML, Hanley HJM, Millat J, Dymond JH, de Castro CN. Transport properties of fluids: Their correlation, prediction and estimation. Cambridge: Cambridge Univ. Press; **1996**.
[18] Huber ML, Laesecke A, Perkins RA. Model for the viscosity and thermal conductivity of refrigerants, including a new correlation for the viscosity of R134a. Industrial & Engineering Chemistry Research **2003**;42(13):3163-78.
[19] Roy D, Thodos G. Thermal conductivity of gases. Hydrocarbons at normal pressures. Industrial & Engineering Chemistry Fundamentals **1968**;7(4):529-34.
[20] Teja AS, Rice P. A generalized corresponding states method for the prediction of the thermal conductivity of liquids and liquid mixtures. Chemical Engineering Science **1981**;36(2):417-22.
[21] Teja AS, Tarlneu G. Prediction of the thermal conductivity of liquids and liquid mixtures including crude oil fractions. The Canadian Journal of Chemical Engineering **1988**;66(6):980-6.
[22] Arikol M, Gürbüz H. A new method for predicting thermal conductivity of pure organic liquids and their mixtures. The Canadian Journal of Chemical Engineering **1992**;70(6):1157-63.
[23] Mathias PM, Parekh VS, Miller EJ. Prediction and correlation of the thermal conductivity of pure fluids and mixtures, including the critical region. Industrial & Engineering Chemistry Research **2002**;41(5):989-99.
[24] Lashkarbolooki M, Hezave AZ, Bayat M. Correlating thermal conductivity of pure hydrocarbons and aromatics via perceptron artificial neural network (PANN) method. Chinese Journal of Chemical Engineering **2017**;25(5):547-54.

[25] Gharagheizi F, Ilani-Kashkouli P, Sattari M, Mohammadi AH, Ramjugernath D, Richon D. Development of a general model for determination of thermal conductivity of liquid chemical compounds at atmospheric pressure. AIChE Journal **2013**;59(5):1702-8.
[26] Hopp M, Gross J. Thermal conductivity of real substances from excess entropy scaling using PCP-SAFT. Industrial & Engineering Chemistry Research **2017**;56(15):4527-38.
[27] Assael MJ, Dymond JH, Papadaki M, Patterson PM. Correlation and prediction of dense fluid transport coefficients: II. Simple molecular fluids. Fluid Phase Equilibria **1992**;75:245-55.
[28] Assael MJ, Dymond JH, Papadaki M, Patterson PM. Correlation and prediction of dense fluid transport coefficients. I. n-alkanes. International Journal of Thermophysics **1992**;13(2):269-81.
[29] Assael MJ, Dymond JH, Patterson PM. Correlation and prediction of dense fluid transport coefficients. V. Aromatic hydrocarbons. International Journal of Thermophysics **1992**;13(5):895-905.
[30] Guo XQ, Sun CY, Rong SX, Chen GJ, Guo TM. Equation of state analog correlations for the viscosity and thermal conductivity of hydrocarbons and reservoir fluids. Journal of Petroleum Science and Engineering **2001**;30(1):15-27.
[31] Fouad WA, Vega LF. Transport properties of HFC and HFO based refrigerants using an excess entropy scaling approach. The Journal of Supercritical Fluids 2018;131:106-16.
[32] Schilling J, Tillmanns D, Lampe M, Hopp M, Gross J, Bardow A. From molecules to dollars: integrating molecular design into thermo-economic process design using consistent thermodynamic modeling. Molecular Systems Design & Engineering 2017;2(3):301-20.
[33] Assael MJ, Dymond JH, Papadaki M, Patterson PM. Correlation and prediction of dense fluid transport coefficients. III. n-Alkane mixtures. International Journal of Thermophysics **1992**;13(4):659-69.
[34] Assael MJ, Kalyva AE, Kakosimos KE, Antoniadis KD. Correlation and prediction of dense fluid transport coefficients. VIII. Mixtures of alkyl benzenes with other hydrocarbons. International Journal of Thermophysics **2009**;30(6):1733-47.
[35] Fareleira JMNA, Nieto de Castro CA, Pádua AAH. Prediction of the thermal conductivity of liquid alkane mixtures. Berichte der Bunsengesellschaft für Physikalische Chemie **1990**;94(5):553-9.
[36] Huber ML. Preliminary models for viscosity, thermal conductivity, and surface tension of pure fluid constituents of selected diesel surrogate fuels. US Department of Commerce, National Institute of Standards and Technology; **2017**.
[37] Ramos-Pallares F, Schoeggl FF, Taylor SD, Yarranton HW. Expanded fluid-based thermal conductivity model for hydrocarbons and crude oils. Fuel **2018**;224:68-84.
[38] Gharagheizi F, Ilani-Kashkouli P, Sattari M, Mohammadi AH, Ramjugernath D, Richon D. Development of a quantitative structure–liquid thermal conductivity relationship for pure chemical compounds. Fluid Phase Equilibria **2013**;355:52-80.
[39] Gharagheizi F, Ilani-Kashkouli P, Sattari M, Mohammadi AH, Ramjugernath D. A group contribution method for determination of thermal conductivity of liquid chemicals at atmospheric pressure. Journal of Molecular Liquids **2014**;190:223-30.
[40] Govender O, Rarey J, Moller BC, Ramjugernath D. A new group contribution method for the estimation of thermal conductivity for non-electrolyte organic compounds; **2016**.

Available from: http://www.ddbst.com/files/files/Durban/SACEC2009-TCN-Manuscript.pdf. [Accessed 4 November 2018].
[41] Nagvekar M, Daubert TE. A group contribution method for liquid thermal conductivity. Industrial & engineering chemistry research **1987**;26(7):1362-5.
[42] Wu KJ, Zhao CX, He CH. Development of a group contribution method for determination of thermal conductivity of ionic. Fluid Phase Equilibria **2013**;339:10-4.
[43] Rodenbush CM, Viswanath DS, Hsieh FH. A group contribution method for the prediction of thermal conductivity of liquids and its application to the Prandtl number for vegetable oils. Industrial & Engineering Chemistry Research **1999**;38(11):4513-9.
[44] Lazzús JA. A group contribution method to predict the thermal conductivity λ (T, P) of ionic liquids. Fluid Phase Equilibria **2015**;405:141-9.
[45] Ramos-Pallares F, Schoeggl FF, Taylor SD, Yarranton HW. Prediction of thermal conductivity for characterized oils and their fractions using an expanded fluid based model. Fuel **2018**;234:66-80.
[46] University OS. Fluid Properties Research Report LV **1983**:25-32.
[47] Kesler MG, Lee BI. Improve prediction of enthalpy of fractions. Hydrocarbon process **1976**;55:153-8.
[48] Gross J, Sadowski G. Perturbed-chain SAFT: An equation of state based on a perturbation theory for chain molecules. Industrial & Engineering Chemistry Research **2001**;40(4):1244-60.
[49] Sauer E, Stavrou M, Gross J. Comparison between a homo- and a heterosegmented group contribution approach based on the perturbed-chain polar statistical associating fluid theory equation of state. Industrial & Engineering Chemistry Research **2014**;53(38):14854-64.
[50] Tamouza S, Passarello JP, Tobaly P, de Hemptinne JC. Group contribution method with SAFT EOS applied to vapor liquid equilibria of various hydrocarbon series. Fluid Phase Equilibria **2004**;222:67-76.
[51] Thi TXN, Tamouza S, Tobaly P, Passarello JP, de Hemptinne JC. Application of group contribution SAFT equation of state (GC-SAFT) to model phase behaviour of light and heavy esters. Fluid phase equilibria **2005**;238(2):254-61.
[52] Rokni HB, Moore JD, Gupta A, M^{c}Hugh MA, Gavaises M. Entropy scaling based viscosity predictions for hydrocarbon mixtures and diesel fuels up to extreme conditions. Fuel **2019**;241:1203-13.
[53] Tihic A, Kontogeorgis GM, von Solms N, Michelsen ML, Constantinou L. A predictive group-contribution simplified PC-SAFT equation of state: application to polymer systems. Industrial & Engineering Chemistry Research **2008**;47(15):5092-101.
[54] Burgess WA, Tapriyal D, Gamwo IK, Wu Y, M^{c}Hugh MA, Enick RM. New group-contribution parameters for the calculation of PC-SAFT parameters for use at pressures to 276 MPa and temperatures to 533 K. Industrial & Engineering Chemistry Research **2014**;53(6):2520-8.
[55] Rokni HB, Gupta A, Moore JD, M^{c}Hugh MA, Bamgbade BA, Gavaises M. Purely predictive method for density, compressibility, and expansivity for hydrocarbon mixtures and diesel and jet fuels up to high temperatures and pressures. Fuel **2019**;236:1377-90.
[56] Laursen T. VLXE, V. 9.3 www.vlxe.com. **2017**.
[57] Rosenfeld Y. Relation between the transport coefficients and the internal entropy of simple systems. Physical Review A **1977**;15(6).

[58] Liang Z, Tsai HL. The vibrational contribution to the thermal conductivity of a polyatomic fluid. Molecular Physics **2010**;108(13):1707-14.
[59] Stiel LI, Thodos G. The self-diffusivity of dilute and dense gases. The Canadian Journal of Chemical Engineering **1965**;43(4):186-90.
[60] Lötgering-Lin O, Gross J. Group contribution method for viscosities based on entropy scaling using the perturbed-chain polar statistical associating fluid theory. Industrial & Engineering Chemistry Research **2015**;54(32):7942-52.
[61] Briggs DKH. Thermal conductivity of liquids. Industrial & Engineering Chemistry **1975**;49(3):418-21.
[62] Dortmund Data Bank (DDB), Thermal Conductivity of Benzene **2018**.
[63] Rastorguev YL, Pugach VV. Untersuchung der wärmeleitfähigkeit von aromatischen kohlenwasserstoffen bei hohem druck. Izv.Vyssh.Uchebn. Zaved, Neft'i Gaz **1970**;13(8):69-72.
[64] Kashiwagi H, Oishi M, Tanaka Y, Kubota H, Makita T. Thermal conductivity of fourteen liquids in the temperature range 298–373 K. International Journal of Thermophysics **1982**;3(2):101-16.
[65] Wada Y, Nagasaka Y, Nagashima A. Measurements and correlation of the thermal conductivity of liquid n-paraffin hydrocarbons and their binary and ternary mixtures. International Journal of Thermophysics **1985**;6(3):251-65.
[66] Wakeham WA, Yu HR, Zalaf M. The thermal conductivity of the mixtures of liquid hydrocarbons at pressures up to 400 MPa. International Journal of Thermophysics **1990**;11(6):987-1000.
[67] Fareleira JMNA, Li SFY, Wakeham WA. The thermal conductivity of liquid mixtures at elevated pressures. International Journal of Thermophysics **1989**;10(5):1041-51.
[68] ASTM International. ASTM D975-18 Standard Specification for Diesel Fuel Oils. West Conshohocken, PA; **2018**.
[69] ASTM International. ASTM D1655-18a Standard Specification for Aviation Turbine Fuels. West Conshohocken, PA; **2018**.
[70] Akhmedova-Azizova LA, Abdulagatov IM, Bruno TJ. Effect of RP-1 compositional variability on thermal conductivity at high temperatures and high pressures. Energy & Fuels **2009**;23(9):4522-8.
[71] Bruno TJ. The Properties of RP-1 and RP-2 MIPR F1SBAA8022G001. **2008**.
[72] Xu GQ, Jia ZX, Wen J, Deng HW, Fu YC. Thermal-conductivity measurements of aviation kerosene RP-3 from (285 to 513) K at sub-and supercritical pressures. International Journal of Thermophysics **2015**;36(4):620-32.
[73] Jia Z, Xu G, Deng H, Jie W, Fu Y. Experimental measurements of thermal conductivity of hydrocarbon fuels by a steady and kinetic method. Journal of Thermal Analysis and Calorimetry **2016**;123(1):891-8.
[74] Bruno TJ. Thermodynamic, Transport and Chemical Properties of Reference JP-8. NIST; **2006**.
[75] Edwards T. "Kerosene" Fuels for Aerospace Propulsion-Composition and Properties. *38th AIAA/ASME/SAE/ASEE Joint Propulsion Conference & Exhibit* Indianapolis, Indiana; **2002**.
[76] Xu R, Wang H, Billingsley M. Thermochemical properties of rocket fuels; **2015**. Available from:

https://web.stanford.edu/group/haiwanglab/HyChem/approach/Report_RP2_Fuel_Thermochemical_Properties_v2.pdf. [Accessed 1 November 2018].
[77] Deng HW, Zhang CB, Xu GQ, Tao Z, Zhang B, Liu GZ. Density measurements of endothermic hydrocarbon fuel at sub-and supercritical conditions. Journal of Chemical & Engineering Data **2011**;56(6):2980-6.
[78] Won SH, Dooley S, Veloo P, Santner JS, Ju Y, Dryer FL. Characterization of global combustion properties with simple fuel property measurements for alternative jet fuels. *50th ASME/SAE/ASEE Joint Propulsion Conference.* Cleveland, OH; **2014,** AIAA 2014-3469.
[79] Chickos JS, Zhao H. Measurement of the vaporization enthalpy of complex mixtures by correlation-gas chromatography. The vaporization enthalpy of RP-1, JP-7, and JP-8 rocket and jet fuels at T= 298.15 K. Energy & fuels **2005**;19(5):2064-73.
[80] Shafer L, Striebich R, Gomach J, Edwards T. Chemical class composition of commercial jet fuels and other specialty kerosene fuels. *14th AIAA/AHI Space Planes and Hypersonic Systems and Technologies Conference* Canberra, Australia; **2006,** AIAA 2006-7972.
[81] Balagurunathan J. Investigation of ignition delay times of conventional (Jp-8) and synthetic (S-8) jet fuels: A shock tube study Ph.D.: University of Dayton; **2012**.
[82] Davidson DF, Zhu Y, Wang S, Parise T, Sur R, Hanson RK. Tube Measurements of Jet and Rocket Fuels. *54th AIAA Aerospace Sciences Meeting.* San Diego, CA; **2016,** AIAA 2016-0178.